

**Near-surface hydrologic response in a fragmented mountainous landscape:
Tat Hamlet, Da River Watershed, northern Vietnam**

Alan D. Ziegler^{1,2*}, Thomas W. Giambelluca², Don Plondke^{2,3}, Thomas T. Vana²,
Jefferson Fox³, Tran Duc Vien⁴, Michael A. Nullet², Steve Evett⁵

¹*Environmental Engineering & Water Resources Program, Princeton University, Princeton NJ 08544 (USA)*

²*Geography Department, University of Hawaii, 2424 Maile Way, Honolulu HI 96822 (USA)*

³*Environmental Studies Program, East-West Center, Honolulu HI 96848 (USA)*

⁴*Center for Natural Resources and Environmental Studies (CRES) of the Vietnam National University, Hanoi*

⁵*USDA-ARS, 2300 Experiment Station Road, Bushland, TX 79012-0010 (USA)*

**corresponding author, adz@princeton.edu; webdata.soc.hawaii.edu/hydrology/*

Abstract

Measurements of saturated hydraulic conductivity and computer simulations of Horton overland flow (HOF) generation are used to assess the effects of landscape fragmentation on near-surface hydrologic response in an upland watershed in northern Vietnam. The fragmented landscape resulting from timber extraction and swidden agriculture is a mosaic of surfaces having unique hydrologic response characteristics. Human disturbance related to these activities has reduced surface infiltrability and altered near-surface flow paths, relative to an undisturbed forest landcover. Roads, paths, and dwelling complexes are highly compacted surfaces capable of generating HOF for small rainfall depths; therefore, these surfaces having relatively small areal extents can contribute disproportionately to basin runoff response. Recently abandoned fields have the lowest surface values of saturated hydraulic conductivity (K_s) of all non-consolidated surfaces tested. Beginning 1-2 years after abandonment, diminished K_s recovers over time with the succession to more advanced types of secondary vegetation. If grassland emerges as the initial replacement vegetation, rather than a bamboo-dominated landcover, the recovery in K_s may occur faster. Distinct reductions in K_s with depth below the surface were also found to be associated with fragmentation. This anisotropy in K_s increases the likelihood of a lateral flow component occurring in the vadose zone. Therefore, for medium-to-large storms the potential for saturation overland flow occurring downslope is increased in the fragmented landscape. The time required for the recovery of subsurface K_s is greater than that for the surface. Thus, the impact fragmentation has on basin hydrologic response may linger well after the surface vegetation has evolved to a mature secondary or forest association. Finally, HOF simulations show that relatively narrow buffers of secondary vegetation are sufficient in reducing overland transport to the stream system during typical seasonal storms. The juxtaposition of various landcover types, therefore, largely determines the influence of fragmentation on basin storm response.

keywords: landcover change, overland flow, runoff generation, watershed surface hydrology, forest fragmentation, SE Asia

1. Introduction

In many mountainous watersheds of Montane Mainland SE Asia (MMSEA), once-forested areas have been replaced by fragmented landscapes composed of remnant forest patches, advanced and emerging secondary vegetation, grasslands, swidden fields (both in use and recently abandoned), tree plantations, and highly compacted surfaces, including roads, paths, and housing complexes. In the Da River Watershed of northern Vietnam, fragmentation results from decades of timber extraction, forest usage by mountain peoples, swidden agriculture practices, and in some cases, revegetation (cf. Cuc and Rambo, 1999). Compared with primary old-growth forest, these fragmented landscapes are degraded, but the resulting hydrological impacts are not yet clearly understood.

Forest removal produces a wide range of hydrological responses (Bruijnzeel, 1990, 2000). In nearby northern Thailand, we've found that various landcover types within fragmented upland watersheds have unique infiltration rates (Ziegler and Giambelluca, 1997; Ziegler et al., 2000, in review). The juxtaposition of all landuse types potentially influences the conveyance efficiency of surface runoff to the stream network. For example, surfaces having low infiltrability, such as paths and roads, act as source areas for Horton overland flow (HOF, rainfall rate in excess of infiltration rate and surface storage) on lands where it is otherwise rare. Other surfaces having high infiltrability may serve as buffers by infiltrating surface runoff generated directly upslope. Detailed knowledge of the spatial arrangement of runoff sources and buffers is therefore important to understanding the conveyance of surface runoff to the stream network.

This field study was directed at increasing understanding of surface runoff in a fragmented landscape within an upland region of northern Vietnam. Herein we (1) quantify saturated hydraulic conductivity on the dominant landcover types, then group the lands having similar infiltration characteristics; (2) verify the susceptibility of each landuse group to HOF generation during typical yearly storms; (3) examine the effects of fragmentation on subsurface hydrological pathways; and (4) investigate the buffering phenomenon, as related to the current spatial distribution of landcover in fragmented study area.

2. Background and Study Area

2.1 Tat Hamlet

The research was conducted near Tat Hamlet (roughly 19:00N, 104:45E) in northern Vietnam (Figure 1). Tat is one of six hamlets comprising Tan Minh Village, which is located SSW of Hanoi, in Da Bac District of Hao Binh Province. The study area is within the Da (Black) River Watershed in a region characterized by sinuous narrow valleys and steep mountains. Elevation is approximately 360 m asl, with surrounding mountain peaks rising to 800-950 m. Of the total 743 ha comprising Tat, 20% has slope < 25 degrees, with only the narrow valley floor being flat enough for permanent settlement, roads, and paddy rice. Mountain slopes are typically 40-60 degrees. The climate is tropical monsoon with hot summer (29.2°C) and cold winter (15°C) seasons. About 90% of the annual 1800 mm of rainfall occurs between May and October. Soils are complex and varied, as parent material is highly variable (sandstone and schist predominate, with some quartz and mica-bearing granite being present). Hillslope soils are acidic, low in nutrients, and contain a high degree of clay. The area was predominately forested until the 1960's, but today remnant patches exist primarily on steep, inaccessible peaks and slopes. Some hilltops and ridgelines are now covered with mature secondary forests. Slopes are often occupied with active swidden fields, farmed by the Tay villagers who primarily inhabit Tat Hamlet. Various stages of young and advanced secondary vegetation (mixtures of grasses, herbs, bamboo, and small trees) are found on former swidden agricultural sites. Field data for this project were collected within a forest fragment and adjacent cleared lands, located on the mountain ridge, immediately above Tat Hamlet.

2.2 Model of hydrologic response for an undisturbed setting

The area encompassing Tat Hamlet has been inhabited for centuries, but only within the last 50+ years has forest removal intensified, creating the fragmented landscape that now exists. While it is impossible to quantify accurately pre-disturbance catchment hydrologic response, some information can be gleaned from the data that will be presented below. For example, HOF generation on a predominantly forested landscape was probably rare because surface infiltrability was high. Figure 2 represents an idealized model of how rainfall was likely partitioned (after Elsenbeer and Vertessy, 2000). Of importance to this study are the high surface infiltration (as indicated by high saturated hydraulic conductivities, K_s) and the reduction in K_s with depth in the subsurface

profile (anisotropy, cf. Elsenbeer and Vertessy, 2000). Based on the data that will be presented later, we believe high K_s values ($>150 \text{ mm h}^{-1}$) extended down into the profile more than 1-1.5m. This magnitude of K_s is great enough to infiltrate rainwater from all but the rarest storms. For large volumes of infiltrating water, abrupt depth-specific reductions in K_s represent depths within the soil profile where some downward-moving water preferentially moves laterally, thereby contributing (potentially) to the generation of saturation overland flow downslope. However, in the pre-disturbance forested scenario, the depth at which this horizontal component was activated (below 1-2m) may have been great enough to prevent SOF from occurring often. The working model of hydrologic flowpaths in Figure 2 serves as a basis for comparison with the surfaces now found in the fragmented landscape of the study area.

3. Methods

3.1 Saturated hydraulic conductivity

Data were collected during short field campaigns in March and June, 1998. Surface bulk density (ρ_b) and antecedent soil moisture (θ_n) were determined by sampling a 5-cm depth with a 90 cm^3 core, then oven drying for 24 h. Saturated hydraulic conductivity and sorptivity values were estimated from infiltration measurements taken *in situ* with Vadose Zone Equipment Corporation (Amarillo, TX) disk permeameters. The permeameter is a modification of the design described by *Perroux and White* (1988). The technique for estimating K_s with this device is described by *Cook et al.* (1993). Use of this instrument in a similar research environment in northern Thailand is explained in *Ziegler and Giambelluca* (1997).

Because the distribution of K_s is not normally distributed (Freeze, 1975 and Dahiya et al., 1984), we used the nonparametric Mann-Whitney U-test (M-W U) during initial statistical analyses to determine if two landuse types had indistinguishable K_s values; the Kruskal-Wallis (K-W) nonparametric ANOVA test was used for landuse groups of three or more. Once major K_s groups were identified, standard ANOVA followed by post-hoc testing with Games-Howell (G-H) test (when P values were significant at $\alpha=0.5$) were used to take advantage of the grouping algorithm in the software (SAS, 1998).

3.2 Rainfall

One-min rainfall intensities were recorded from 26 March to 29 June 1998 using a MET-ONE (Grants Pass, OR) tipping bucket raingauge and data logger. This period encompassed the transition from the dry to rainy season. Storm events were defined based on the criteria of Wischmeier and Smith (1978): a precipitation event accumulating at least 12.7 mm without a 6-h rain-free period, or an event having at least 6.4 mm within any 15-min period. During low intensity periods, rainfall can accumulate for more than one-min in the 0.254 mm tipping bucket before it is recorded (one-click) by the logger. We therefore corrected the raw data set by distributing the first 0.254 mm, recorded following a rain-free period, equally among each preceding minute.

3.3 Infiltration calculations

Steady-state infiltration is calculated using a modification of the *Philip* (1957) infiltration equation:

$$f_{ss} = \frac{1}{2} S t^{-\frac{1}{2}} + C K_s \quad [1]$$

where S and K_s are respectively median field-measured sorptivity and saturated hydraulic conductivity. As the limit of time approaches ∞ , f_{ss} approaches the final term, which is an approximation of the steady state infiltration rate. In the original equation (*Philip*, 1957), the final term is simply stated to be a value approximately K_s . The coefficient C is added to acknowledge the final value is likely less than the soil K_s . Following *Loague and Freeze* (1985), we used a value of 0.5 in prior research in Thailand (*Ziegler and Giambelluca*, 1997). Herein, we again use $C = 0.5$ to estimate steady-state infiltration rates for comparison with measured one-min rainfall intensities.

3.4 Hillslope field HOF simulations

A suite of computer simulations using the KINEROS2 runoff model (*Smith et al.*, 1995, 1999) were conducted to assess how the spatial arrangement of the various landcover types influences hydrologic response during storms. The simulations were directed at quantifying the reduction of surface runoff to the stream system that results from having a non-agricultural buffer (of various length) between an agricultural field and a downslope stream. We

simulated the situation where a 30x30m field is located immediately above a buffer ranging in length from 2 to 160m. Figure 3 presents an overview of the simulations. ABANDONED FIELD was used for the 30x30m field because it is the most hydrologically active agricultural surface we found in the study area (i.e., has the lowest K_s). The downslope landcovers were ABANDONED FIELD (considered to be a control) and the three dominant replacement vegetation types found in the study area: GRASSLAND, YOUNG SEC VEG, and INTERMEDIATE SEC VEG (referred to as buffers, described below).

3.4.1 General description of the KINEROS2 model

KINEROS2 is an event-based, physics-based runoff and erosion model (Smith *et al.*, 1995, 1999). Dynamic, distributed flow modeling in KINEROS2 is well-suited to describe HOF generation and transport for hillslope-scale simulations. Horton overland flow simulation in KINEROS2 utilizes the kinematic wave method to solve the dynamic water balance equation:

$$\frac{\partial h}{\partial t} + \frac{\partial Q}{\partial x} = q(x,t) \quad [2]$$

where h is water storage per unit area, $Q(x,t)$ is water discharge, x is distance downslope, t is time, and $q(x,t)$ is net lateral inflow rate. Solution of Eq. 2 requires estimates of time- and space-dependent rainfall $r(x,t)$ and infiltration $f(x,t)$ rates:

$$q(x,t) = r(x,t) - f(x,t) \quad [3]$$

The infiltration model in KINEROS2 utilizes several parameters describing a one- or two-layer soil profile: K_s , integral capillary drive or matric potential (G), porosity (f), and pore size distribution index (I). The coefficient of variation for K_s can be specified to account for spatial variation in infiltration. Inclusion of two soil layers allows modeling a restrictive surface or subsurface layer. The general one-layer infiltrability (f_c) model is a function of cumulative infiltration (I):

$$f_c = K_s \left[1 + \frac{\mathbf{a}}{e^{(\mathbf{a}/B)} - 1} \right] \quad [4]$$

where \mathbf{a} is a parameter related to soil type (fixed at 0.85 in KINEROS2) and $B = (G + h_w)(Q_s - Q_i)$, for which h_w is surface water depth and the second term, unit storage capacity, is the difference of effective saturation (Q_s) and soil moisture (Q_i).

Hillslopes in KINEROS2 are treated as a cascading network of surface, channel, and pond elements. Channels receive flow from adjacent surfaces or upslope channels. Rectangular surfaces may be cascaded or arranged in parallel to represent complex topography as in Figure 3b). Each element is characterized by assigning parameter values that control runoff generation, e.g., K_s and an index of antecedent soil moisture. Dynamic, distributed flow modeling in KINEROS2 requires a temporal record of rainfall rate.

3.4.2 KINEROS2 parameterization and calibration for the buffer simulations

Prior to simulation, KINEROS2 was calibrated using rainfall simulation data obtained from small-scale plot experiments on an abandoned upland rice field in northern Thailand (Ziegler et al., in review). The Thailand field was similar to the ABANDONED FIELD surface in Tat in terms of surface K_s , soil properties, and vegetation characteristics (e.g., coverage, height, interception, age since usage). The thick line in Figure 3c shows the KINEROS2 prediction of the measured Thailand rainfall simulation runoff time series (represented by the open circles). Resulting total error (E_{total}), error in the peak estimate (E_{peak}), and root mean squared error ($RMSE$) for the KINEROS2 prediction were acceptably <1%, 4.5%, and 16.7%, respectively. Buffer simulations were performed by replacing KINEROS2 parameter values from the Thailand calibration simulations with those obtained from field measurements in Vietnam (e.g., surface K_s , slope, saturation, interception, percent cover, and porosity). The parameters for the buffer simulations are shown in Table 1. A common representation for the lower soil layer was used for all buffer simulations because we did not have data to quantify these parameters for the four simulated landcovers.

4. Results

4.1 Surface and subsurface K_s

After taking into consideration land use, major vegetation structure, and infiltrability, we identified seven hydrologically distinct landcover classes (Table 2). Descriptive statistics of K_s for each type are listed in Table 3; mean values with similar letter superscripts are not statistically different (ANOVA, G-H, $\alpha = 0.05$). Figure 4 shows box plots of K_s for five of the seven landuse types. Box widths bracket the approximate age when the vegetation type appears on the landscape following cultivation/swiddening until it gives way to a more advanced replacement vegetation. Of note is the dramatic reduction in K_s beginning at time of abandonment, followed by a slow recovery in infiltrability, which is dependent on the type of replacement secondary vegetation cover (evident in the means). The speckled area shows the 25-75th percentiles for the GRASSLAND cover.

Figure 5 shows box plots of K_s over four depths for four locations (Stations 301-304, defined in Section 6). Means and standard deviations are presented in Table 4. The 0-m values in Figure 5 correspond to the surface values listed in Table 3: FOREST for sites 302 and 303; YOUNG SEC VEG for site 304; and UPLAND FIELD for site 301. The yellow shading and dotted lines highlight the 25-75th percentile range of the forest data—it is presented in the graphs of the other sites for comparison.

4.2 Rainstorms

Of a total of 49 rainfall events recorded during the collection period, only 11 were classified as storms. Duration, total and average rainfall, and maximum intensity for these 11 storms are shown in Table 5. The storms are ranked from largest (STORM 1) to smallest (STORM 11). Rankings were determined by first ranking the events separately according to total rainfall, average rainfall, and maximum rainfall intensity subcategories. The final rankings were based on the sum of the three rankings, i.e., the largest event had the smallest sum of ranks.

4.3 Indicators of HOF generation potential

Table 6 shows the percentage of one-min intensities for each of the 11 storms that are greater than the mean K_s on the seven major landuse types. In Figure 6, the one-min rainfall intensity times series for the 6 largest storms are plotted with time-dependent infiltration rates, calculated with Eq. 1 using measured K_s and sorptivity data for each landuse class. Periods where rainfall exceeds infiltration represent times when HOF could be generated.

4.4. Buffer simulations

Results of the buffer simulations for the five largest events are shown in Table . For each storm, total rainfall (mm), KINEROS2-predicted HOF on the 30x30m field (mm), and total simulation time (min) are shown below the storm identifier. For each event, we performed control simulations in which the buffer landcover was ABANDONED FIELD (i.e., the same as the 30x30m upslope field). The predicted runoff values for this control simulation are presented as depths (mm). For the corresponding buffer simulations, the KINEROS2-predicted values are fractions of the depths predicted in the control simulations. For example, during STORM 1, the 2-m grassland buffer treatment produced 2.6 mm of runoff, which is 80% of the 3.2 mm predicted in the control simulation (hence the value 0.8 is presented).

5. Discussion

5.1 Spatial distribution of K_s

Preliminary reconnaissance conducted prior to the field study revealed that the landscape was a mosaic of forest (mostly secondary), various stages of secondary vegetation (including re-emerging trees mixed with stands of bamboo and understory vegetation, grasslands, and shrublands), upland fields (cultivated, slashed, abandoned/fallow), and disturbed surfaces (paths, roads, hut complexes). Our sampling strategy was to collect data for as many landcover subtypes as possible. In order to determine the classes listed in Table 2, preliminary statistical analyses of K_s values within the various subtypes were performed (discussed below). Following ANOVA testing on the major classes, three general groups appeared (ranked from lowest K_s to highest): {CONSOLIDATED}, {YOUNG SEC VEG, FALLOW FIELD}, and {UPLAND FIELD, FOREST, GRASSLAND}, with ADVANCED SEC VEG overlapping with the latter two groups.

The two youngest replacement landcover types (i.e., replacing a cultivated or abandoned field), GRASSLAND and YOUNG SEC VEG, were determined to have different K_s during ANOVA testing ($\alpha = 0.05$), despite both covers having many common grasses (Table 2). In the preliminary analyses, these two surfaces were also judged to be unique using the nonparametric Mann-Whitney U-test. However, the tied P-value was equal to our cutoff criteria of 0.050. We separated the two because observations showed that the soil matrix underlying the GRASSLAND surface had properties associated with higher permeability (e.g., lower bulk density, greater

aggregation, A more dense root structure) than that under the YOUNG SECONDARY VEG sites. We concluded that some of our measurements may also have been affected by trampling, and that a larger sample population would likely show stronger statistical support that they are indeed different. In support, the box plots in Figure 7a show convincing evidence of dissimilarity; statistical testing for the small sample sizes was undoubtedly influenced by a few outliers.

Although FOREST K_s was among the highest of all landcover types, it is probably lower than what would be expected in an undisturbed setting (i.e., Figure 2). In support, K_s at a depth of 0.1 m was more than twice as high (roughly 220 versus 90 mm h^{-1} ; recorded near Station 303, Table 4) as the surface value. Our surface measurements for this landcover seem to have a low bias that may result from the sampling methodology. Most forested lands in the study area were excluded from testing because they occur predominantly on steep slopes where access is difficult. Furthermore, use of the permeameters on these lands would have required disturbing the surface by leveling. Thus, many forest K_s measurement sites were likely disturbed by human/animal trampling, which consolidates the surface, thereby reducing K_s . In fact, approximately half of the measurements were taken at the forest edge, where K_s was generally found to be lower than in the interior (Figure 7c). Lower K_s values at the forest edge may also result from trampling or edge-versus-interior vegetation differences, which affect variables that control infiltration (e.g., macro-porosity, organic matter, understory cover density, throughfall rates). We grouped the interior and edge values to form the FOREST class even though statistical analyses provided weak evidence that they may be different (M-W U; Tied-P value was 0.0491). In the general description of hydrological pathways for the historical forest landcover (Figure 2), we minimize the low bias in the FOREST estimate by choosing a range of K_s that is in line with the 0.1-m depth values at Station 303.

5.2 Temporal controls on K_s

Surface K_s in the fragmented landscape changes temporally over both short and long scales. For example, immediately following hoeing (for planting or weeding), K_s on agricultural fields is the highest of all landcover types—except, perhaps, a truly undisturbed forest. Prior to the commencement of the 1998 rainy season, median K_s on the upland field was 127 mm h^{-1} ($n = 8$). As shown in Figure 7b, median K_s had declined to 95 mm h^{-1} ($n = 9$) only a few weeks later during the rainy season (Tied P-value = 0.0543, M-W U). Rainfall impact, and other surface-disruption processes that breakdown or disperse fines into open surficial pores (e.g., walking, wind,

settling), likely contribute to the reduction in K_s on this short time scale. Unfortunately, our sampling strategy only allows detection of this change, but not derivation of a predictable relationship with time, rainfall, or mechanical phenomena. Nevertheless these data demonstrate that *surface preparation*, and its ensuing effects on infiltration, can produce different hydrologic responses for similar storm events, much like differing values of antecedent soil moisture would.

We also found a significant reduction in K_s on agricultural lands beginning about the time of abandonment. The ABANDONED FIELD surface, approximately 6-9 months following harvesting, had the lowest K_s values of any non-consolidated surface (22 mm h⁻¹; Table 3). In northern Thailand, we similarly found that K_s on cultivated fields dropped from 350 mm h⁻¹ to 130 mm h⁻¹ in the six months following abandonment (Ziegler et al., in review); Giambelluca (1996) earlier found a similar response in Brazil and Thailand, as did Chandler and Walter (1998) in the Philippines. At the Vietnam site, a distinct replacement vegetation (e.g., YOUNG SEC VEG in Table 2) emerges in about 1-2 years following abandonment, fostering an increase in K_s . Eventually, as this vegetation matures, K_s increases toward a value represented by INTERMEDIATE SEC VEG, and then FOREST. This long-term (> 10-15 years) recovery in K_s is depicted in Figure 4. As an alternative to this relatively slow regeneration, if the GRASSLAND cover type becomes the initial replacement vegetation, K_s may recover faster (shown by the shading in Figure 4). Currently the evolution from one replacement cover to another is not well understood. It is however, generally believed that the GRASSLAND landcover is undesirable because it inhibits succession back to tree-dominated landcover types (Cuc and Rambo, 1999).

5.3 Hydrologic flowpaths

Subsurface K_s values support that human disturbance in the study area has altered the subsurface hydrology. This likely results from a combination of factors, including changes in vegetation type (e.g., changes rooting depth), surficial compaction extending down into the profile, and surface lowering (i.e., deeper soil layers with reduced K_s are brought closer to the surface). The box plots in Figure 5 show that each of the three disturbed landcovers have subsurface K_s values that are much lower than those determined at the forest site (303). The effect this may have on the downward flow of infiltrating water is illustrated in Figure 8, and can be compared with the conceptual model presented in Figure 2. The FOREST (303, interior) description is essentially the same as that in Figure 2, except that surface K_s is slightly lower, owing to the factors discussed above. At a depth of about 0.5

m, reduction in K_s becomes apparent. However, K_s is still in excess of 100 mm h^{-1} , a rate that is probably great enough to infiltrate rainwater from all but the rarest storms; surface runoff generation is therefore probably not affected greatly. This is likely not the case for the other surfaces, where both surface and subsurface K_s are low. Lower surface K_s dictates that HOF would be generated for smaller rainfall depths. Distinct reductions in K_s occurring from 0.1-0.4m below the surface indicate that for large storms a lateral flow component could be produced, thereby increasing the likelihood of saturation overland flow occurring downslope.

The conceptual models of hydrologic pathways for agricultural and secondary vegetation lands illustrate the potential consequences of fragmentation on runoff generation. In both cases, K_s reductions occurring at relatively shallow depths are probably great enough to produce substantial lateral flow components during storms of moderate-to-large duration and rainfall intensity (e.g., Storm 3, Table 5, Figure 6). The influence of this anisotropy is dependent on the specific storm characteristics, location of the surface on a hillslope (e.g., what is landcover downslope?), and the geomorphological pattern of the landscape (i.e., this would not be relevant in low-relief landscapes with a wide amplitude in seasonal groundwater level changes; cf., Elsenbeer and Vertessy, 2000). Although we do not quantify the contribution of a lateral flow component, it is important enough to recognize its existence, and to acknowledge that it may be linked closely to the landscape fragmentation phenomenon. It also reinforces that knowledge of surface K_s is not sufficient in determining the hydrologic impacts of fragmentation and other land disturbance. This point is illustrated in the FOREST EDGE (302) data, where the reduction in K_s is very distinct, as compared with the FOREST (301) site. While variability in soil properties (both soils are Ultisols) may partially explain the differences, age (since disturbance) may be a more accurate determinant. For example, while the FOREST (303) site is located in the center of a remnant forest fragment, the FOREST EDGE (302) site is adjacent to a swidden field. This landcover may be better described as advanced secondary vegetation; and the corresponding low subsurface K_s reflects the historical disturbance (i.e., agriculture), which may include lowering. If this is true, then the vegetation-induced recovery of K_s , as shown in Figure 4, may only apply to the surface; a longer period of time may be required for the entire near-surface profile to recover to pre-disturbance levels. Thus, alterations of subsurface flowpaths that result from human disturbance, may remain long after the surface vegetation has matured.

5.4 Surface runoff generation

Comparing measured one-min rainfall intensities to mean K_s values shows the potential of HOF generation on each of the seven major landcover classes (Tables 6). During the 11 storms, very few one-min intensities exceeded K_s on UPLAND FIELD, FOREST, and GRASSLAND, suggesting HOF generation on these lands is rare. On the two secondary vegetation lands, YOUNG SEC VEG and INTERMEDIATE SEC VEG, one-min values exceeding mean K_s were also generally uncommon. For two storms (2 and 5), however, more than 10% of the one-min intensity values were greater than mean K_s on YOUNG SEC VEG. In contrast, roughly 15 to 50% of the one-min intensities during six of the seven largest storms exceeded mean K_s of the CONSOLIDATED class. Also apparent in Table 6, is the susceptibility of HOF generation on FALLOW FIELD surfaces, compared with UPLAND FIELD.

Within the CONSOLIDATED SURFACE group, K_s values for roads, paths, and dwelling complexes were indistinguishable during preliminary analysis (K-W; Tied P-value = 0.373). K_s on path surfaces ranged from about 4 to 43 mm h^{-1} ; and the median value was 12.6 mm h^{-1} . Roads and hut complexes had smaller ranges and lower median values, 6.8 and 6.2, respectively. These data compare well with those collected in northern Thailand, where path, road, and dwelling complex K_s values are also much lower than any other surface typically found in upland watersheds (Ziegler et al., in review). Although CONSOLIDATED surfaces often represent a small areal proportion of the landscape (estimated at less than 1% in Tat), they potentially contribute disproportionately to storm runoff hydrographs because (1) low K_s allows generation of HOF during most rainfall events, and (2) conveyance efficiencies to the stream channel are usually high, owing to connectivity of the surfaces (especially roads and paths) and proximity to the stream network (especially hut complexes). In Tat Hamlet, road runoff predominantly drains directly into the stream channel. Also of interest is the role of footpaths in acting as source areas for HOF, thereby increasing the surface flow during storms and contributing to accelerated erosion, especially on upland fields where HOF may otherwise be rare (observed in the field during storm 2).

The propensity of some of the landcover types to generate HOF is shown in the instantaneous infiltration plots in Figure 6. This comparison shows periods of high rainfall intensity, an important rainfall characteristic because HOF generation not only requires rainfall greater than K_s , but rainfall intensity must be sustained above some critical threshold. For example, in STORM 6, seven one-min periods exceed the infiltration on

ABANDONED FIELD. These periods are, however, spread over a 30-min period. Therefore, the sustained rainfall intensity may not be great enough to generate HOF, as ponded surface water may be absorbed during the intermediate low-intensity periods. In contrast, STORM 5 contains several consecutive periods where one-min rainfall intensity is greater than the estimated ABANDONED FIELD infiltration, indicating a greater chance of HOF generation. Although Figure 6 and Table 6 are not directly comparable, they both show (1) the likelihood of HOF generation on CONSOLIDATED surfaces in general, (2) the propensity of ABANDONED FIELD and YOUNG SEC VEG landcovers to generate HOF during large storms, and (3) the unlikelihood of HOF occurring on UPLAND FIELD, FOREST, and GRASSLAND surfaces.

5.5 Importance of landscape patterns

The Tat landscape is a mosaic of surfaces having unique infiltrability characteristics. Consequently, unique patterns of overland flow generation potential exist. In general, the implication this has on basin storm response largely depends on the degree of fragmentation, the age (since active use) of the various landcover types, and the juxtaposition of the landcover types within the basin. When assessing near-surface hydrologic response during rain events, one must consider conveyance of surface water to the stream system. Although we don't have sufficient data to perform distributed modeling of the basin hydrologic response, the buffer simulations show the influence that the arrangement of landcover surfaces has on the conveyance efficiency. For most events, narrow buffers of young-to-intermediate secondary vegetation are sufficient to reduce the conveyance of overland flow to the stream systems (Table 7). During the largest simulated event (Storm 1), buffers of 80 m or more reduced runoff to less than 10% of the expected value. Figure 9 shows the buffering effect for the GRASSLAND treatment during STORM 1. These simulation results suggest that if such buffers are positioned (whether intentionally or not) between disturbed lands and riparian zones, some impacts resulting from accelerated HOF can be mitigated. Within a fragmented landscape in general, some buffering occurs by chance. One is tempted to hypothesize that in such an environment (as opposed to the scenario of clear-cut timber removal) that remnant forest fragments act as buffers, having the capacity to infiltrate large volumes of runoff generated upslope. It is then plausible that this might limit basin stormflow response changes caused by increases in HOF generation. In Tat, however, forest fragments appear to be located predominantly at the highest hillslope locations. Their ability to act as buffers, therefore, may be reduced—they do undoubtedly play a role in absorbing runoff generated on

rock outcrops and other terrain with high rock content and shallow soil depths. We are currently investigating this phenomena in detail.

6. Conclusions

Fragmentation has created a mosaic of surfaces that are hydrologically different. The primary activities that lead to fragmentation, timber extraction and swidden agriculture, reduce the saturated hydraulic conductivity in the near-surface soil profile. This reduction leads to an increase in the likelihood of HOF generation, and possibly an increase of other “fast” runoff mechanisms, such as saturation overland flow, during large storms. The hydrologic effects of the former are most noticeable during the period immediately following cultivation or timber harvesting, then decrease over time as various stages of secondary vegetation emerge, bringing about a recovery in infiltration capacity. In general, the more advanced the replacement vegetation, the higher the infiltrability of the surface, and the less likely for the surface to produce HOF. With respect to the latter process, the subsurface profiles beneath both active agricultural lands and replacement vegetation show noticeable reductions in saturated hydraulic conductivity with depth, compared with an undisturbed forest stand. Large decreases in K_s are capable of creating a lateral subsurface flow component—which is probably unusual in undisturbed forests—that can contribute to the generation of saturation overland flow immediately downslope. This effect on subsurface flow partitioning does not recover as rapidly as that of reduced surface infiltration. Even in advanced forms of secondary vegetation having high surface infiltrability, the effects of reduced subsurface K_s may linger, contributing to an accelerated surface flow response well after the above-ground vegetation structure might suggest otherwise.

Currently in the study area, most upland fields extend down to riparian zone. Little thought is given to preventing HOF from draining directly into the stream network. Relatively narrow buffers (5-20m) of a replacement vegetation may be sufficient to infiltrate water generated upslope on fields or footpaths. Grasslands, which are considered to be an undesirable landcover because hinder the succession of tree-dominated associations, are probably the most abundant and efficient buffers within the Tat landscape. However, they are not used intentionally in this capacity. Forest fragments may have a reduced role on mitigating the transport of overland flow to the stream system because they tend to be located on peaks and ridges, above the surfaces where the accelerated runoff is created.

Finally, consolidated surfaces such as roads, footpaths, and housing complexes contribute disproportionately to stormflow response because they have very low infiltrability and are often linked directly to the stream system. These highly disturbed surfaces are inherently a part of the current fragmentation phenomenon. Any success in keeping these surfaces areas to a minimum and/or reducing the conveyance efficiency of overland flow generated on them from reaching the stream system, will reduce the cumulative hydrological impacts of landscape fragmentation.

7. Acknowledgments

This paper results from joint work conducted by researchers from the University of Hawaii, East-West Center (Honolulu, HI), and Center for Natural Resources and Environmental Studies (CRES) of the Vietnam National University, Hanoi. Financial support was provided by a National Science Foundation grant (no. DEB-9613613); Alan Ziegler was supported by an Environmental Protection Agency STAR fellowship. We thank the following for support during the project: Lon, Lian, Mai, and Da (field work), Le Trong Cuc, Dao Minh Truong, Nghiem Phuong Tuyen, Dr. Wang Hu (vegetation identification), and the other CRES staff in Hanoi; Stephen Leisz (GIS and remote sensing); and finally, the Tay villagers who welcomed us in their community.

8. References

- Baruah, P. C. 1973. An investigation of drop size distribution of rainfall in Thailand. Ph.D. dissertation. Asian Institute of Technology, Bangkok, Thailand.
- Bruijnzeel, L.A. 1990. Hydrology of moist tropical forest and effects of conversion: A state of knowledge review. UNESCO, Paris and Vrije Universiteit Amsterdam.
- Bruijnzeel, L.A. 2000. Forest Hydrology. In J.C. Evans (ed.), *The Forestry Handbook*. Blackwell Scientific, Oxford, UK.
- Chandler, D.G., and Walter, M.F. 1998. Runoff responses among common land uses in the uplands of Matalom, Leyte, Phillippines. *Transactions of the ASAE* 41(6): 1635-1641.
- Cook, F.J., G.P. Lilley, and R.A. Nunns. 1993. Unsaturated hydraulic conductivity and sorptivity: laboratory measurement. In M.R. Carter, Ed., *Soil Sampling and Methods of Analysis*. Baco Raton, FL: CRC Press, Inc.
- Cuc, Le Trong and A. Terry Rambo. 1999. Composite Swidden Farmers of Ban Tat: A Case Study of the Enviromental and Social Conditions in a Tay Ethnic Minority Community in Hoa Binh Province, Vietnam. Research Report 1, Center for Natural Resources and Environmental Studies (CRES), Vietnam National Univeristy, Hanoi. 191 p.
- Dahiya, I.S., J. Richter, and R.S. Malik. 1984. Soil spatial variability: a review. *International Journal of Tropical Agriculture* 2: 1-102.
- Elsenbeer, H, Vertessy, R.A. 2000. Hydrologic flowpaths in tropical rainforest soilscaapes—a review. *Hydrological Processes* 14 (14): 2367-2381
- Fox, J., Troung, D.M., Rambo, A.T., Tuyen, N.P., Cuc, L.T. and Leisz, S. 2000. Shifting cultivation: a new paradigm for managing tropical forests. *Bioscience* 50(6):1-8.
- Freeze, R.A. 1975. A stochastic-conceptual analysis of one-dimensional groundwater flow in nonuniform homogeneous media. *Water Resources Research* 11: 725- 741.
- Giambelluca, T.W. 1996. Tropical land cover change: Characterizing the post-forest land surface. In T.W. Giambelluca and A. Henderson-Sellers (eds.), *Climate Change: Developing Southern Hemisphere Perspectives*. John Wiley and Sons, UK, pp. 293-318.
- Gilbert, G.O. 198 *Statistical methods for environmental pllution monitoring*. Van Nostrad Reinhold Co, New York.
- Loague, K.M., and R.A. Freeze. 1985. A comparison of rainfall-runoff modeling techniques on small upland catchments. *Water Resources Research* 21: 229-248.
- Perroux, K.M. and I. White. 1988. Designs for disc permeameters. *Soil Science Society of America Journal*. 52: 1205-1215.
- Philip, J.R. 195 The theory of infiltration: 1. The infiltration equation and its solution. *Soil Science* 83: 345-35
- SAS. 1998. *Staview 5.0.1 User Manual*. Statview Institute Inc., Cary, NC.
- Smith RE, Goodrich DC, Quinton JN. 1995. Dynamic, distributed simulation of watershed erosion: the KINEROS2 and EUROSEM models. *Journal of Soil and Water Conservation* 50 (5): 517-520.

- Smith RE, Goodrich DC, Unkrich CL. 1999. Simulation of selected events on the Catsop catchment by KINEROS2
A report for the GCTE conference on catchment scale erosion models. *Catena* 37: 457-475.
- Wischmeier, W.H., and D.D. Smith. 1978. *Predicting Rainfall Erosion Losses*. Agriculture Handbook no. 53
USDA, Washington D.C.
- Ziegler, A.D. and Giambelluca, T.W. 1999 Importance of rural roads as source areas for runoff in mountainous
areas of northern Thailand. *Journal of Hydrology* 196 (1/4): 204-229.
- Ziegler, A.D., R.A. Sutherland, and T.W. Giambelluca. 2000. Runoff generation and sediment transport on
unpaved roads, paths, and agricultural land surfaces in northern Thailand. *Earth Surface Processes and
Landforms* 25 (5): 519-534.
- Ziegler, A.D., R.A. Sutherland, T.W. Giambelluca. In review. On the trail of erosion: the importance of footpaths
in accelerating Horton overland flow in an agricultural watershed in Northern Thailand. *Geomorphology*

Table 1. Parameters used for the buffer simulations with KINEROS2.

Surface type	K_s^\dagger (mm h⁻¹)	Cv (-)	n (ft^{1/6})	Ca (-)	Int mm
30x30m FIELD	27	0.40	0.13	0.50	0.25
GRASSLAND (buffer)	91	0.48	0.24	0.90	2.00
INT SEC VEG (buffer)	65	0.74	0.20	0.75	1.75
YOUNG SEC VEG (buffer)	41	0.65	0.20	0.75	1.75

[†]Variables are saturated hydraulic conductivity, the coefficient of variation for K_s , Manning's n, vegetation coverage, interception depth, respectively; for all surfaces, the following variables were the same: depth of upper soil layer (0.50 m), layer-2 K_s (41.1 mm h⁻¹), capillary drive (61.93 mm), initial soil saturation index (0.39), porosity (0.54 cm³ cm⁻³), slope (0.84 m m⁻¹), and volumetric rock fraction (1%).

Table 2. Vegetation characteristics of the seven major landuse types in Tat Hamlet[†]

Landcover	Area (ha)	Description
FOREST (includes advanced secondary vegetation)	142	Intensely used secondary evergreen broadleaf forest, attaining heights of 25-30m. The discontinuous upper (25-30m) and complex secondary (8-25m) stories include the following representative tree species: <i>Acanthopanax fragrans</i> , <i>Aleurites montana</i> , <i>Alphonsea tonkinensis</i> , <i>Euodia triphylla</i> , <i>Garcinia planchonii</i> , <i>Ostodes paniculata</i> , <i>Pithecellobium clypearia</i> , and <i>Schefflera octophylla</i> . A bushy understory (2-8m) and the forest floor includes species <i>Antidesma fordii</i> , <i>Breynia angustifolia</i> , <i>Bridelia hermandii</i> , <i>Cyperus nutans</i> , <i>Dioscorea depauperata</i> , <i>Ervatamia cambodiana</i> , <i>Ervatamia bonii</i> , <i>Ficus variegata</i> , <i>Livistona saribus</i> , <i>Miscanthus japonicus</i> , <i>Ostodes paniculata</i> , <i>Phrynium capitatum</i> , <i>Psychotria rubra</i> , and <i>Selaginella monospora</i> .
INTERMEDIATE SECONDARY VEGETATION	171	One-story “forest” dominated by <u>nua</u> (<i>Neohouzeaua dullooa</i> var. 1&2) and <u>giang</u> (<i>Dendrocalamus patellaris</i>) bamboo. Representative species include <i>Alpinia</i> sp., <i>Aleurites monata</i> , <i>Cyperus nutans</i> , <i>Livistona saribus</i> , <i>Pteris vittata</i> , and <i>Styrax tonkinensis</i> . The understory is primarily composed of bamboo litter and shoots emerging from extensive root systems.
YOUNG SEC	181	Evergreen broadleaf bush mixed with <u>nua</u> bamboo occurring in areas where forest was once cleared. Representative species include <i>Acacia pennata</i> , <i>Cyperus nutans</i> , <i>Ervatamia cambodiana</i> , <i>Eupatorium odoratum</i> , <i>Ficus</i> sp., <i>Microstegium vagans</i> , <i>Neohouzeaua dullooa</i> , <i>Saccharum spontaneum</i> , and <i>Urena lobata</i> .
UPLAND FIELD	20	Active swidden fields, including corn (<i>Zea mays</i> L.), banana (<i>Musa coccinea</i> , <i>Musa paradisiaca</i>), and cana (<i>Cana edulis</i> Ker). Other “weedy” vegetation volunteering include <i>Ageratum conyzoides</i> , <i>Eupatorium odoratum</i> , <i>Euphorbia hirta</i> , <i>Gynura crepidioides</i> , <i>Imperata cylindrica</i> , <i>Melia aderazach</i> , <i>Rorippa indica</i> , <i>Saccharum spontaneum</i> , <i>Setaria palmifolia</i> , <i>Solanum erianthum</i> , and <i>Urena lobata</i> . Bare ground is approximately 30-50%.
ABANDONED FIELD	41	Short grass and shrub lands occurring on abandoned fields or lands where frequent grazing has prevented tall vegetation from occurring. Species include <i>Helicteres angustifolia</i> , <i>Imperata cylindrica</i> , <i>Microstegium vagans</i> , <i>Miscanthus japonicus</i> , <i>Paspalum conjugatum</i> , <i>Rorippa indica</i> , <i>Saccharum spontaneum</i> , <i>Litsea cubeba</i> , and <i>Mallotus alba</i> .
GRASSLAND	157	Tall grasslands occurring where forest has been cleared and the land overworked during farming. Three species dominating this landcover, <i>Imperata cylindrica</i> , <i>Thysanolaena latifolia</i> , and <i>Saccharum spontaneum</i> , often reach heights exceeding 2-2.5m and have extensive root systems that help them regenerate quickly after fire. Other common species are <i>Eupatorium odoratum</i> , <i>Microstegium vagans</i> , and <i>Urena lobata</i> .
RICE PADDY	18	Not studied in detail; comparable to general descriptions in other studies.
CONSOLIDATED SURFACES	7 [†]	Highly compacted surfaces including roads, paths, and dwelling sites. Little or no vegetation exists on these frequently used surfaces.
TOTAL	737	

[†] Vegetation descriptions are based on identifications by CRES botanists.

Table 3 Descriptive statistics for K_s and bulk density for seven major landuse groups.

Landcover type	n [†] -	Mean K_s ^{††} (mm h ⁻¹)	K_s Range (mm h ⁻¹)	Median K_s (mm h ⁻¹)	BD (Mg m ⁻³)
UPLAND FIELD	17	112 ± 79 c	23-334	103	0.95 ± 0.08
FOREST	15	91 ± 85 c	12-290	63	0.94 ± 0.10
GRASSLAND	11	90 ± 43 c	14-173	93	1.11 ± 0.10
INTERMEDIATE SEC VEG	8	65 ± 48 bc	9-129	67	1.01 ± 0.06
YOUNG SEC VEG	13	41 ± 27 b	10-103	33	0.95 ± 0.08
ABANDONED FIELD	11	22 ± 11 b	14-45	28	1.06 ± 0.09
CONSOLIDATED SURFACE	32	11 ± 90 a	2-43	7	1.45 ± 0.21

[†] n is sample size, the means are ± one standard deviation, BD is the mean bulk density ± one standard deviation.

^{††} Mean values with same letters indicate no statistical difference, ANOVA (G-H, $\alpha = 0.05$).

Table 4. K_s at three subsurface depths at four locations.

depth (m)	301 [†]	302	303	304
0.1	27 ± 18	30 ± 8	222 ± 163	56 ± 19
0.4	18 ± 12	48 ± 20	117 ± 124	41 ± 19
0.7	43 ± 18	20 ± 24	116 ± 109	30 ± 13

[†] Landcover for sites 301-304 are forest, forest edge, secondary vegetation, and agricultural field, respectively (Figure 5); mean values are ± one standard deviation, n = 4 for each sample.

Table 5. Eleven storm events recorded during the study period (ranked from largest to smallest).

Event [†]	Start (m:d:y:h:mm)	End (m:d:y:h:mm)	Duration (min)	Total (mm)	Average (mm min ⁻¹)	Maximum (mm min ⁻¹)
1	6/4/98 17:21	6/5/98 4:46	686	66.8	0.10	1.8
2	5/18/98 17:15	5/18/98 18:02	48	14.2	0.30	2.3
3	6/9/98 16:03	6/10/98 1:04	542	38.6	0.07	1.3
4	5/31/98 16:16	5/31/98 22:44	389	21.8	0.06	2.0
5	5/28/98 15:03	5/28/98 17:18	136	30.7	0.23	1.0
6	5/5/98 15:22	5/5/98 17:20	119	16.5	0.14	1.8
7	6/7/98 16:06	6/7/98 17:31	86	18.3	0.21	1.0
8	5/23/98 23:31	5/24/98 15:24	954	42.4	0.04	0.8
9	5/19/98 9:48	5/20/98 8:16	1349	31.0	0.02	1.3
10	5/30/98 23:24	5/31/98 7:11	468	16.8	0.04	1.3
11	6/10/98 20:45	6/11/98 4:44	480	14.5	0.03	1.3

[†]Data set extends from 3/26/98 to 6/29/98.

Table 6. Percentage of one-min rainfall values exceeding landuse K_s .

Landcover types	Storms [†]										
	1	2	3	4	5	6	7	8	9	10	11
UPLAND FIELD	0	2	0	0	0	0	0	0	0	0	0
FOREST	1	8	0	1	0	2	0	0	0	0	0
GRASSLAND	1	8	0	1	0	2	0	0	0	0	0
INTERMEDIATE SEC VEG	1	13	0	1	0	3	0	0	0	0	0
YOUNG SEC VEG	4	15	4	3	10	5	9	0	1	0	1
ABANDONED FIELD	7	17	6	4	24	7	24	1	1	0	2
CONSOLIDATED SURFACE	15	33	14	7	49	22	41	8	5	6	5

[†]Storms are ranked from largest to small; storm statistics are shown in Table 5.

Table 7. Runoff predictions for the buffer simulations during five largest storms using KINEROS2

Events [†]	Width (m)	Downslope landcover			
		Control ABAN FIELD (mm)	GRASSLAND (mm:mm)	INT SEC VEG (mm:mm)	YOUNG SEC VEG (mm:mm)
Storm 1	2	3.2	0.8*	0.8	0.9
RF: 66.8 mm	5	3.2	0.6	0.7	0.8
Field HOF: 3.25 mm	10	3.2	0.5	0.7	0.8
Sim time: 746 min	20	3.2	0.2	0.4	0.6
	40	3.2	0.0	0.2	0.3
	80	2.7	0.0	0.1	0.1
	160	2.2	0.0	0.1	0.1
Storm 2	2	0.02	0.5	1.0	1.0
RF: 14.2 mm	5	0.02	0.5	1.0	1.0
Field HOF: 0.01 mm	10	0.02	0.5	1.0	1.0
Sim time: 108 min	20	0.02	0.5	0.5	1.0
	40	0.01	1.0	1.0	2.0
	80	0.01	0.0	1.0	2.0
	160	0.01	0.0	0.0	2.0
Storm 3	2	0.1	0.1	0.4	0.6
RF: 38.6 mm	5	0.1	0.2	0.5	0.7
Field HOF: 0.05 mm	10	0.1	0.1	0.3	0.6
Sim time: 602 min	20	0.2	0.1	0.2	0.3
	40	0.2	0.1	0.2	0.3
	80	0.1	0.1	0.2	0.3
	160	0.1	0.1	0.3	0.4
Storm 4	2	0.2	0.1	0.2	0.3
RF: 21.8 mm	5	0.2	0.2	0.2	0.2
Field HOF: 0.30 mm	10	0.2	0.2	0.2	0.2
Sim time: 449 min	20	0.2	0.2	0.3	0.3
	40	0.2	0.2	0.2	0.3
	80	0.1	0.2	0.3	0.4
	160	0.1	0.1	0.3	0.3
Storm 5	2	0.15	0.3	0.4	0.5
RF: 30.7 mm	5	0.14	0.3	0.4	0.5
Field HOF: 0.28 mm	10	0.15	0.2	0.3	0.4
Sim time: 196 min	20	0.16	0.3	0.3	0.3
	40	0.20	0.2	0.2	0.2
	80	0.18	0.1	0.2	0.2
	160	0.14	0.0	0.1	0.1

[†]Event information includes storm number (Table 5), total rainfall, KINEROS2-predicted HOF from the 30x30m field (ABANDONED FIELD, no buffer), and total KINEROS2 simulation time.

* For each storm and respective buffer length, GRASSLAND, INT SEC VEG, and YOUNG SEC VEG values are percentages of the simulated runoff for ABAN FIELD control simulation (e.g., the starred value is calculated as $RO_{GRASSLAND} / RO_{ABAN_FIELD}$, or $0.8 = 2.6 \text{ mm} / 3.2 \text{ mm}$). The simulation schematic is shown in Figure 3.



Figure 1. Tat Hamlet. The study area in northern Vietnam.

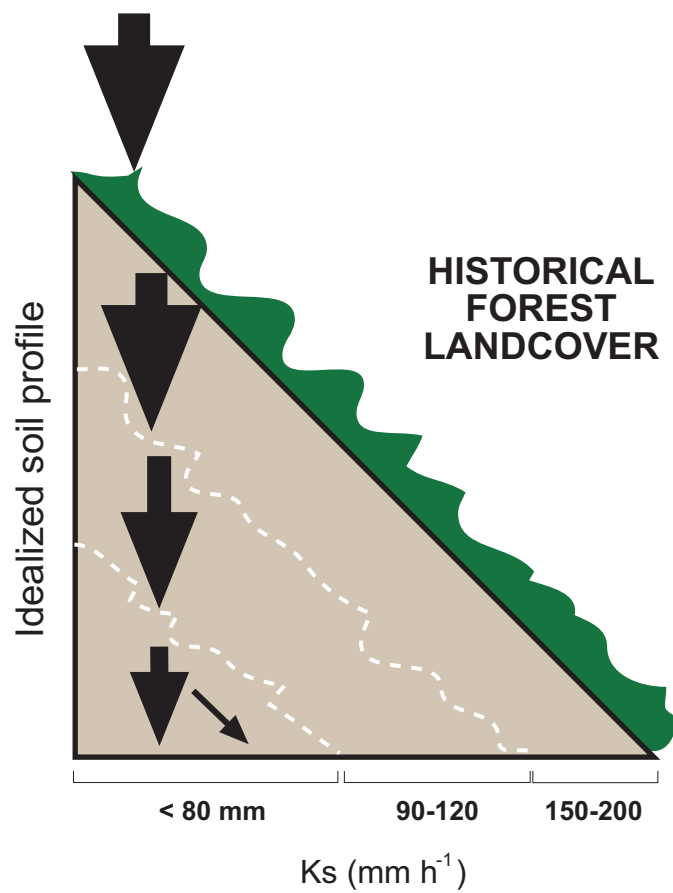


Figure 2. Generalized model of vertical and lateral flowpaths of infiltrating rainwater for the historical forested landscape. Values of saturated hydraulic conductivity (K_s) are based on data collected in this study. Note surface K_s is high enough to infiltrate rainwater from all but the rarest rain events.

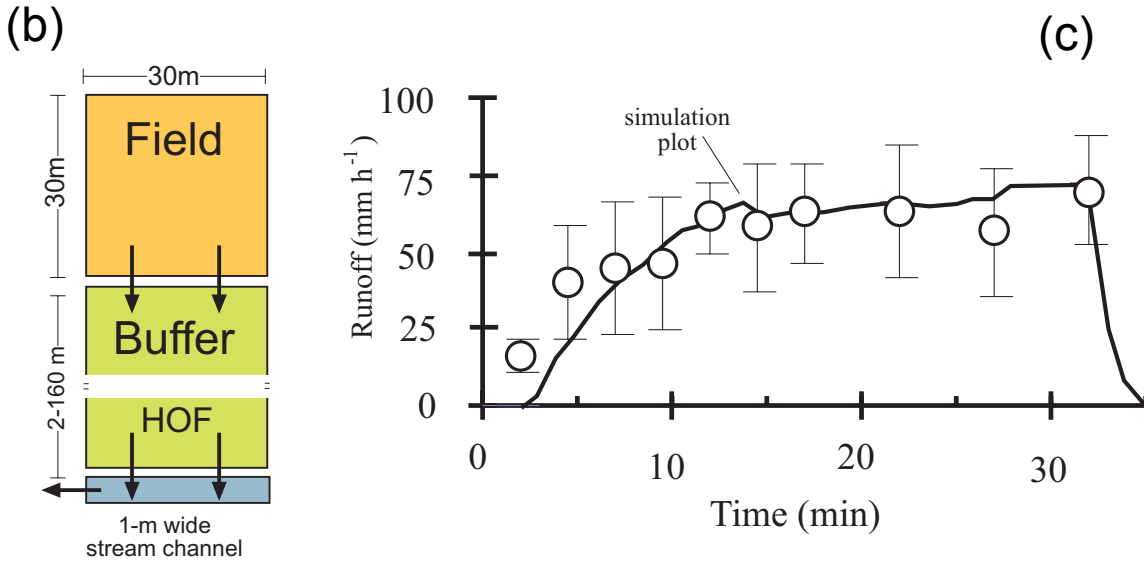
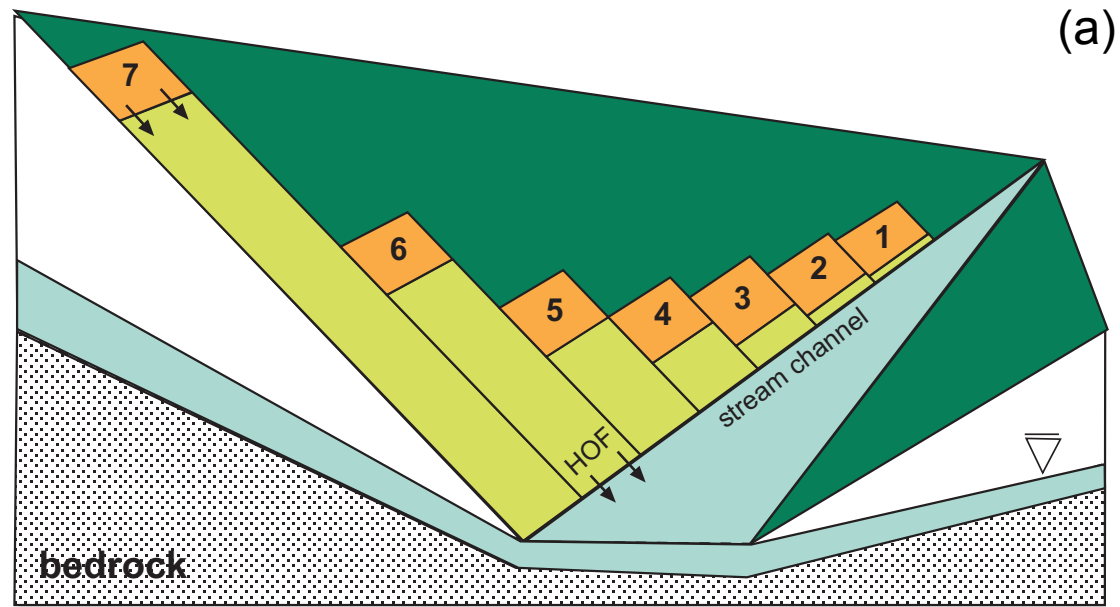


Figure 3. (a) Schematic for the buffer simulation using KINEROS2. (b) Each simulation consisted of a 30x30m upslope field, with a 2- to 160-m wide buffer immediately downslope, above the stream channel; vegetation types for the buffer treatment were GRASSLAND, YOUNG SEC VEG, and INT SEC VEG (Table 2). (c) KINEROS2 was calibrated using field rainfall simulation data from a Thailand experiment on similar soils and landcovers (from Ziegler et al., 2000, in review). Comparison of observed runoff during field rainfall simulation experiments (open circles) with the KINEROS2-predicted time series (thick black line) is shown here. The Vietnam buffer simulations were performed by replacing the KINEROS2 parameters for the Thailand calibration simulations with those determined at the Tat Hamlet field site.

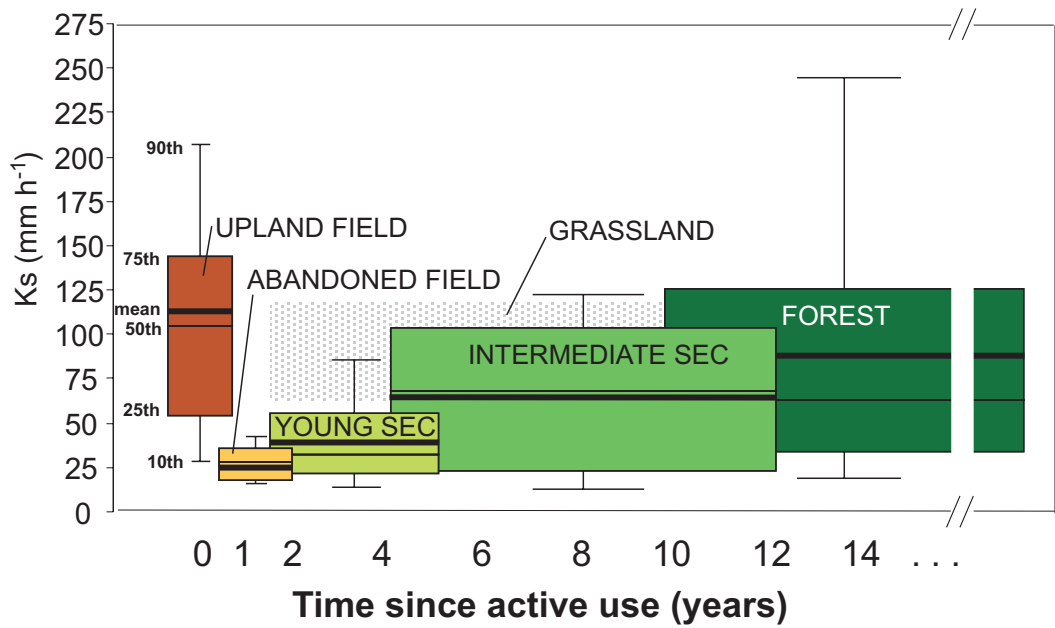


Figure 4. Boxplots of saturated hydraulic conductivity (K_s) for five landcover types. Box widths correspond to approximate times each cover type exists on the landscape before being replaced by a more advanced cover type. The X-axis represents the time since active cultivation/swiddening. GRASSLAND represents a young/intermediate cover that increases infiltrability more quickly than the other types of replacement vegetation of the same approximate age.

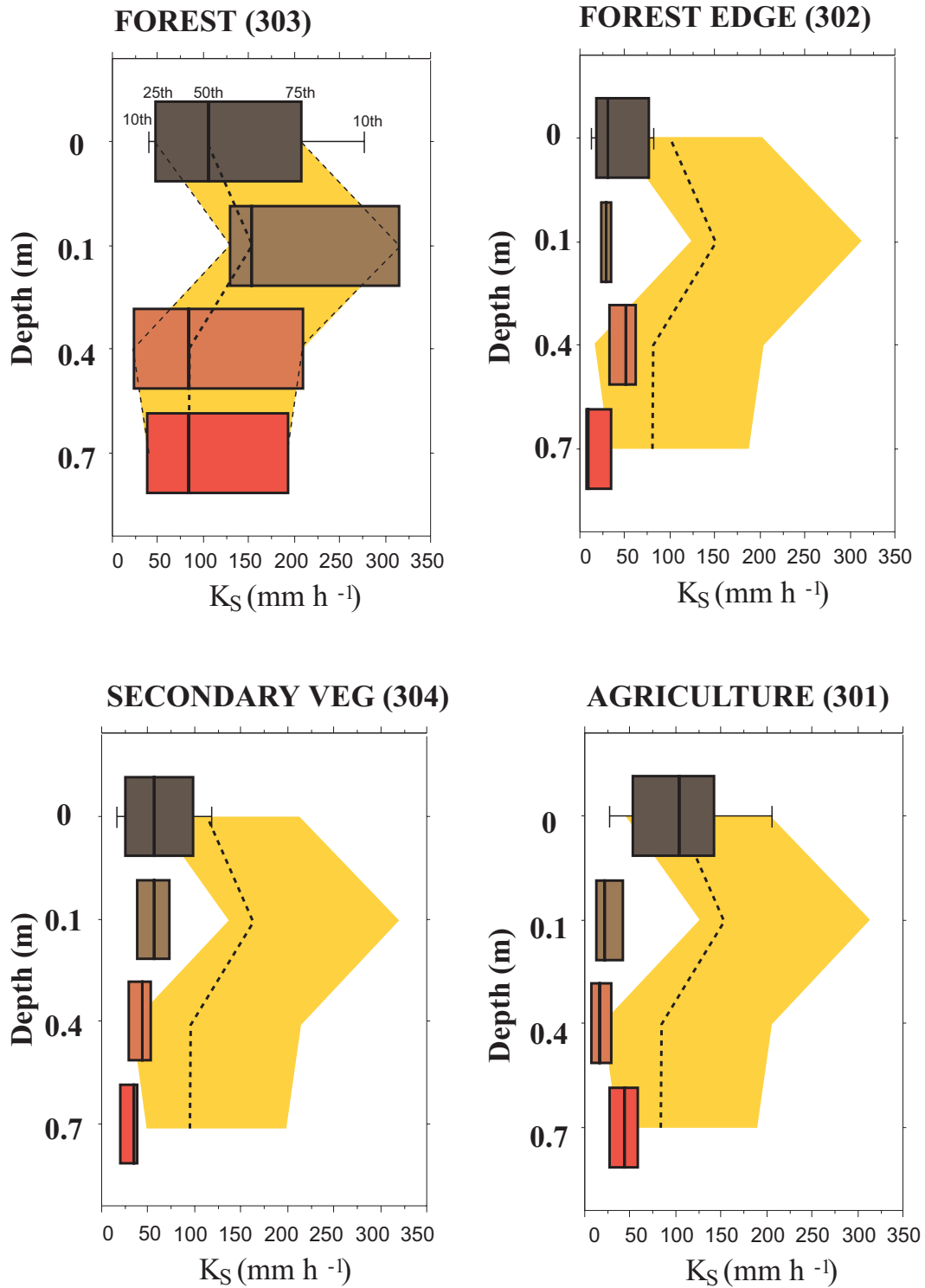


Figure 5. Box plots of saturated hydraulic conductivity (K_S) data at several depths for four locations. The highlighted area and dotted lines show the 25-75th percentile range for the data at the forest (303) site. This information is provided in the background of each of the other three sites for comparison.

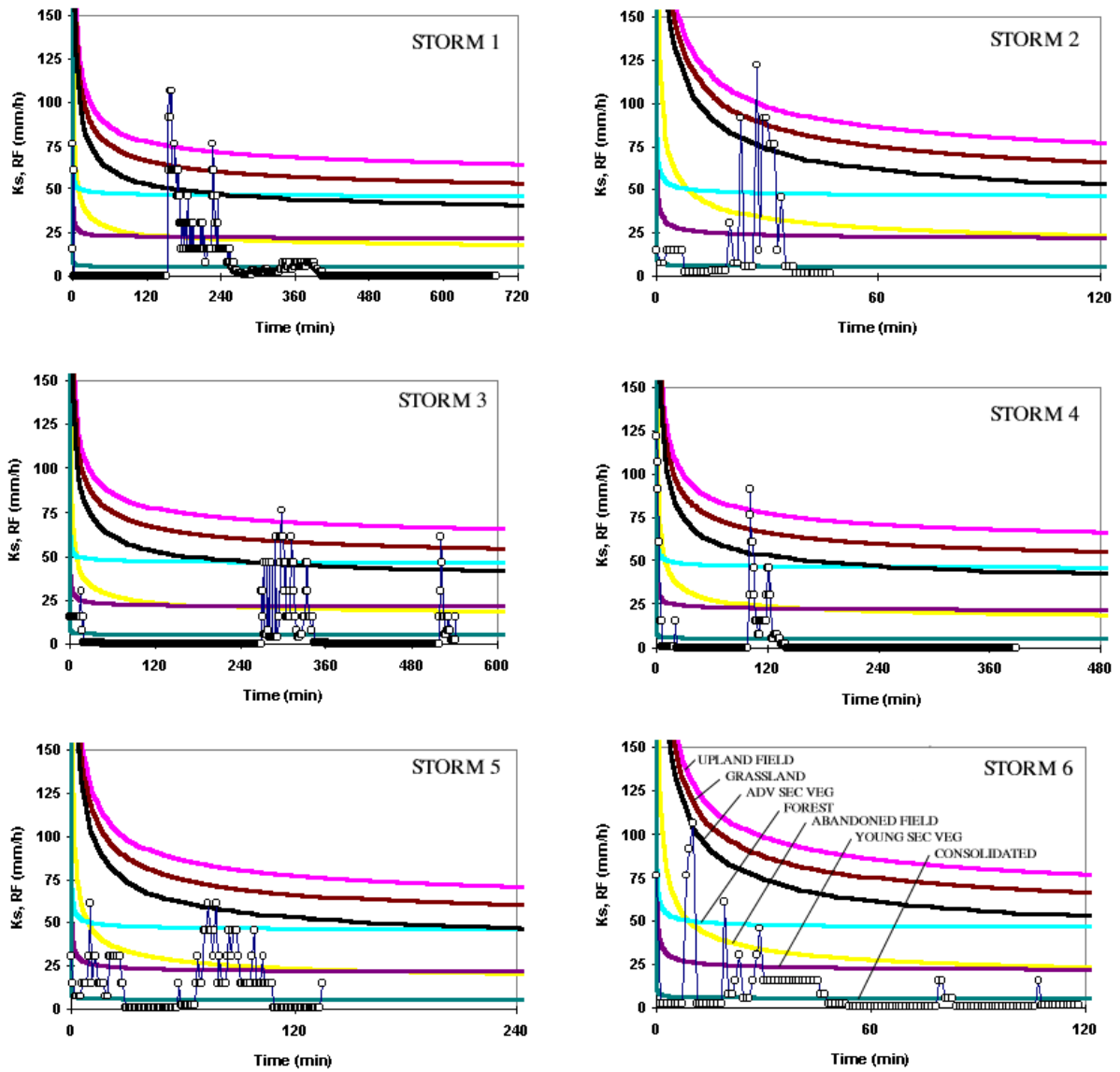


Figure 6. One-min rainfall intensities for six storms plotted against time-varying infiltration rate, calculated with Eq. 7.1 and field measured values of saturated hydraulic conductivity and sorptivity. The tags in the STORM 6 plot apply to all storms.

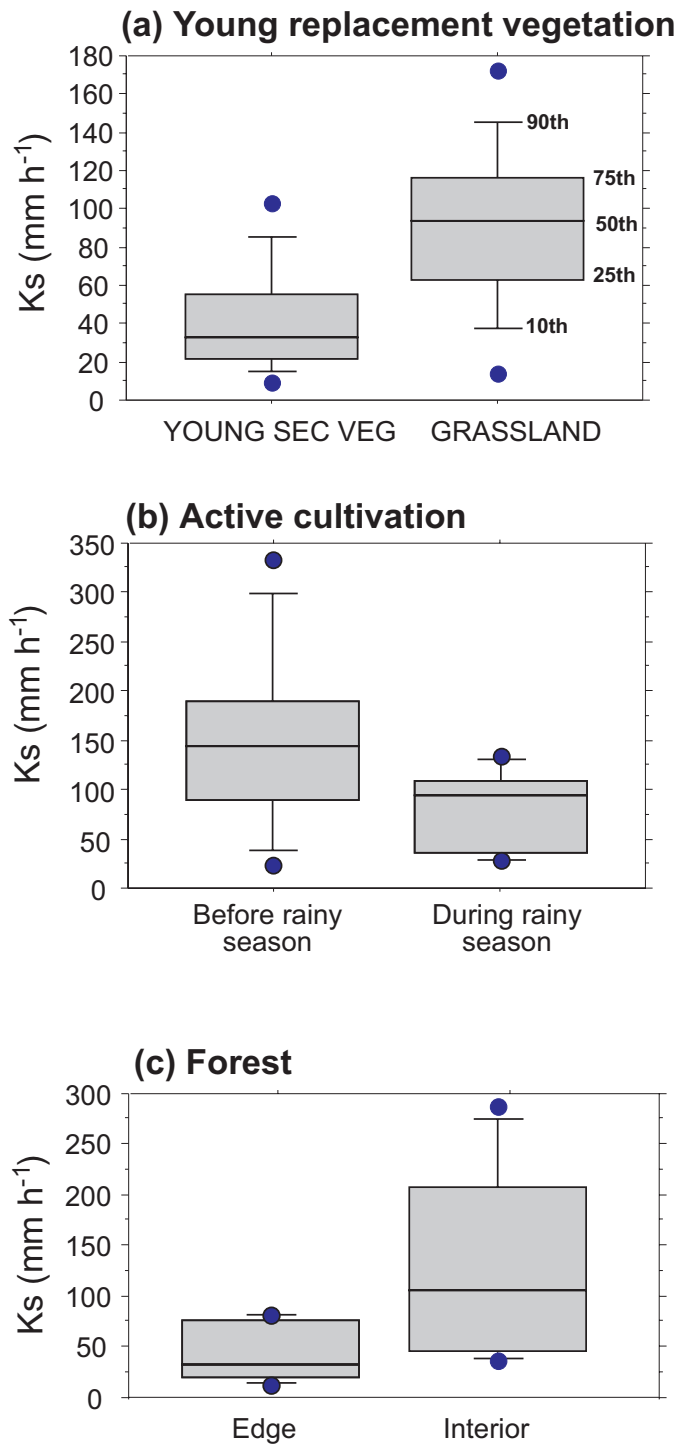


Figure 7. Box plots of saturated hydraulic conductivity (K_s) for several pairs of surfaces that were investigated prior to determining the final seven major landuse types listed in Table 2.

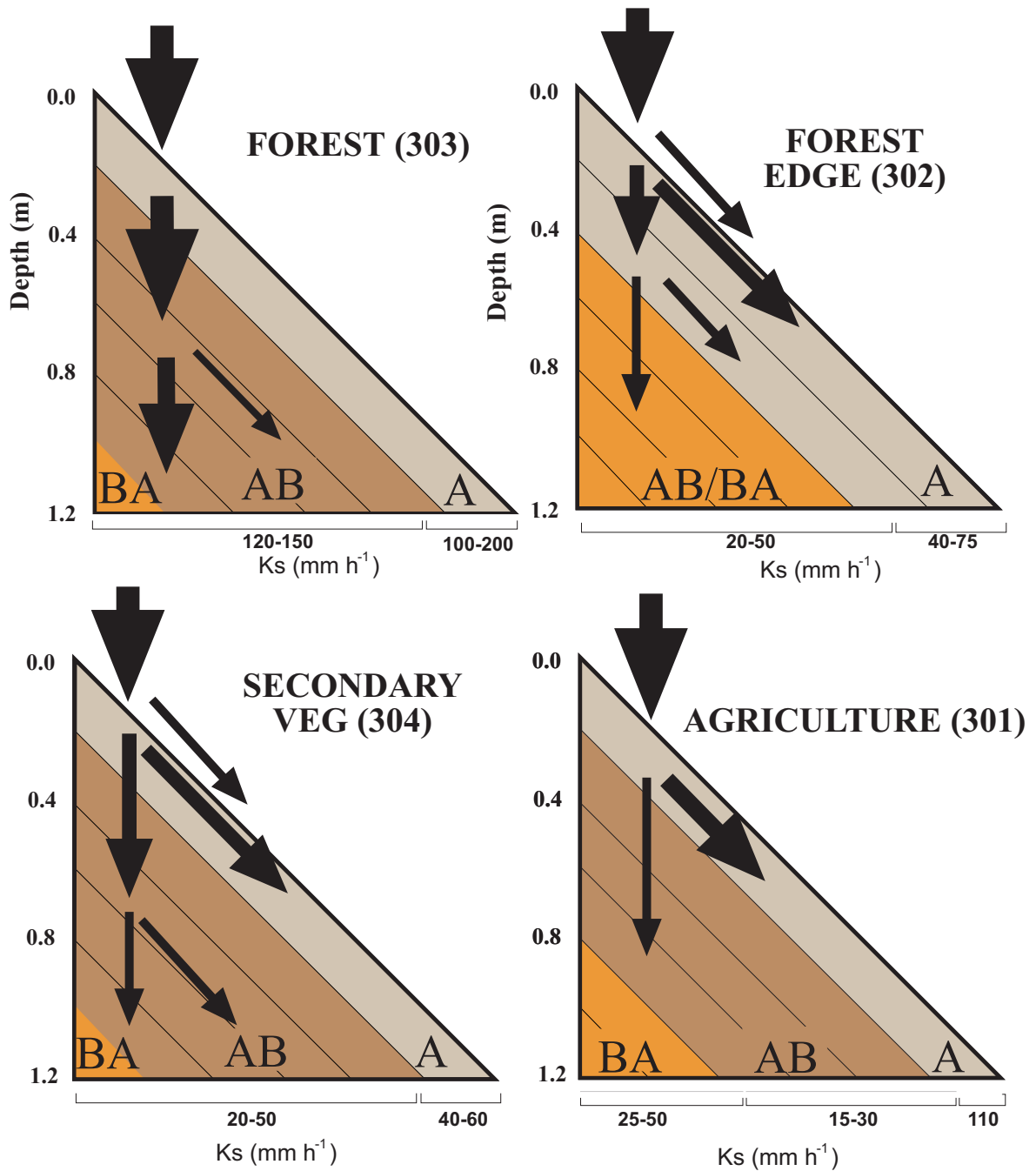


Figure 8. Conceptual model of the partitioning of infiltrating rainwater at four locations. In general, the size of the arrows indicates the proportion of water “taking” a vertical or lateral flow direction. Lateral flow is produced by abrupt reductions in K_s within the soil profile. Arrows above the land surface represent Horton overland flow. Letters and color changes for each soil profile show the transitions between soil horizons. The generalized ranges of K_s are estimated from the field data (Tables 3,4; Figure 7).

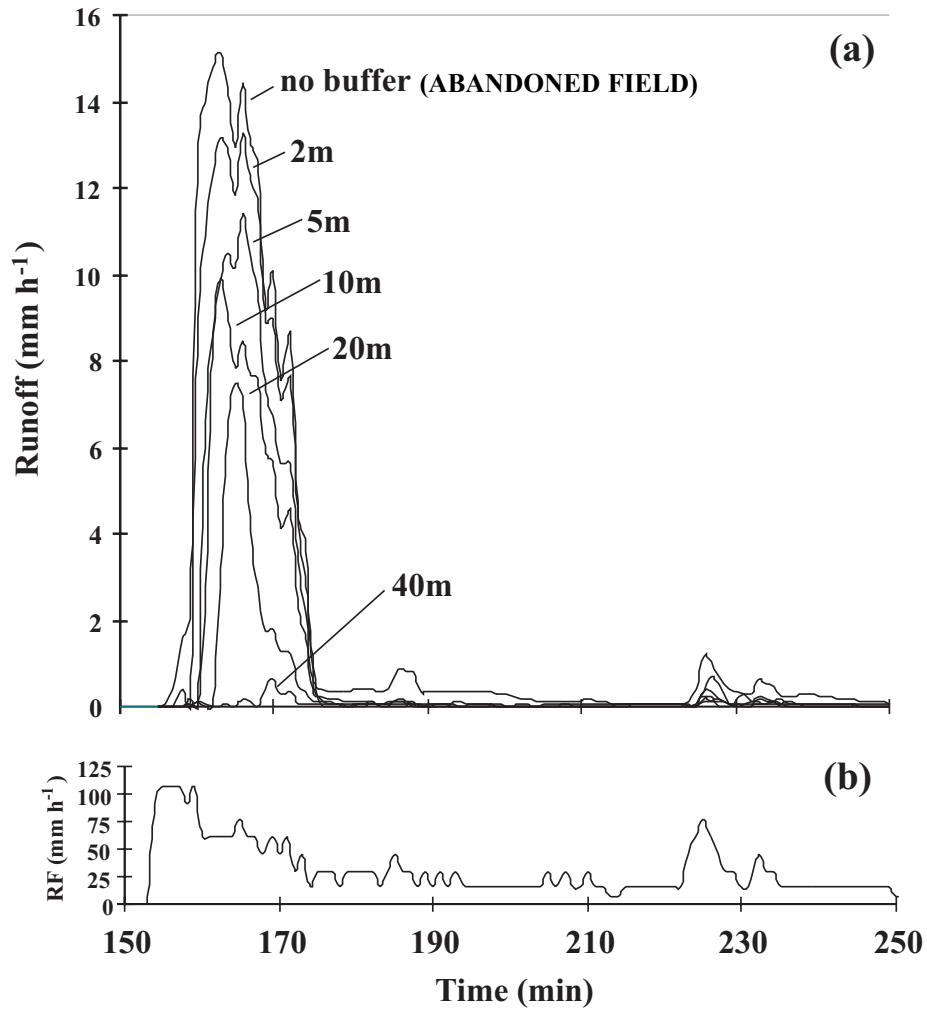


Figure 9. (a) KINEROS2-simulated runoff during STORM 1 for the GRASSLAND buffer treatment. The buffer time series is compared with that of the ABANDONED FIELD control simulation. (b) The corresponding rainfall time series period during which HOF was produced.